ELSEVIER

Journal of Nuclear Materials 253 (1998) 167–174

journal of nuclear materials

Radiation-induced electrical degradation: an effect of surface conductance and microcracking

W. Kesternich *

Institut für Festkörperforschung, Forschungszentrum Jülich, and Association FZJ-Euratom, Postfach 1913, D-52425 Jülich, Germany

Abstract

Single and polycrystalline Al_2O_3 specimens have been irradiated by 28 MeV alpha particles at 450 and 500°C in an electric field of 350 kV/m. Increases and decreases of the electrical surface conductance, depending on the irradiated specimen area, have been observed, but no changes of the volume conductivity. The two contrary effects of irradiation on the surface conductance are explained by surface diffusion of hydrocarbon molecules. Large increases of the apparent volume conductivity under irradiation were observed as a result of microcracking. Scanning electron microscopy is proposed as a sensitive tool for microcrack detection. By changing the irradiation parameters, the microcracks could be sealed and the pre-irradiation conductivity restored. Thus internal and external surface conductances may both be radiation-enhanced. Implications for the design of electrically insulating fusion reactor components are expected. © 1998 Elsevier Science B.V.

1. Introduction

In electrically insulating materials irradiation causes increases of the electrical conductivity due to creation of electron–hole pairs [1,2]. This so-called radiation-induced conductivity (RIC) is nearly proportional to the dose rate, and the conductivity recovers close to its pre-irradiation value when the irradiation is terminated. In addition to RIC a permanent degradation of the electrical resistivity of ceramic insulator materials has been reported [2], investigated in detail for electron irradiation by Hodgson et al. [3–7] and Zong et al. [8–10], and confirmed for proton and neutron irradiation by Pells et al. [11,12] and Shikama et al. [13,14], respectively. The experiments [4] indicated that this so-called radiation-induced electrical degradation (RIED) occurred only when irradiation is performed under the presence of an electric field and in a temperature window between about 250 and 550°C. Since the conductivity increases ranged to observed values as high as 0.1 S/m in Al_2O_3 (as compared to intrinsic conductivities of about 10^{-14} to 10^{-12} S/m) and may possibly extend far beyond this value with further dose increase, RIED is expected to pose a severe problem for the application of ceramic insulators in various fusion reactor components. In 1993, however, Kesternich et al. [15] showed that RIED-like effects can be caused by surface leakage currents in various types of ceramic insulators due to carbon contamination of the specimens, that such contaminations are enhanced by irradiation, and that on the other hand no RIED could be observed when special precautions were taken against such contamination effects. Surface effects as the origin of apparent RIED have also been observed by other research groups [16–18]. The question was raised [15] whether all results, which attribute RIED to increases of the volume conductivity, were caused by artifacts.

In the present work an experiment has been carried out which reveals that RIED-like conductivity increases can also arise when microcracks are present in the ceramic specimens, and that the occurrence of such conductivity increases depends on the irradiation condition. The significances of radiation-induced conductances along surfaces and through microcracks are discussed.

* Fax: +49-2461 612 410.

PII S0022-3115(97)00324-3

2. Experimental details

Specimen platelets of dimension 7.5×7.5 mm^2 with truncated corners were prepared by diamond wheel sawing from single crystalline (Commercial Crystal Laboratories, $\langle 0001 \rangle$ orientation) and polycrystalline Al_2O_3 (Rubalit 710 by Hoechst and Vitox (Deranox grade) by Morgan and Matroc). The specimens of original thicknesses between 0.5 and 1 mm were thinned down to between 150 and 170 μm by grinding with 40 μm diamond paste. Both specimen faces were polished using successively 15, 6, and 3 μm diamond paste and finally a suspension of 0.25 μm SiO_2 powder. The specimens were brazed onto 3-5 mm thick specimen holders consisting of pure nickel or an Fe–Co–Ni alloy of type Vacon70. Brazing was carried out using a Ag–4Ti brazing foil at 1000°C or an Ag–Cu–In–Ti foil at 950°C in vacuum of better than 1×10^{-5} Torr with subsequent very slow cooling through the temperature range from 960°C (melting temperature) down to 500°C in the case of Ag–Ti and correspondingly from 780 to 430°C in the case of Ag–Cu–In–Ti.

Subsequently a central electrode of 5 mm diameter and a concentric guard electrode of about 6 mm inner and 7 mm outer diameters were sputter-deposited onto the top surface of the specimen. The electrodes consisted of 0.3 μm Ti followed by 2 μm Au layers. The opposite (bottom) electrode consisted of the brazing foil. After cleaning, the surface resistances between central and guard and between guard and bottom electrode were > 2 GΩ at 450°C. Two 100 μm thick Au contact wires were spot-welded to each of the two top electrodes. Using two contact wires each, allowed measurement of the electrical lead plus contact resistances which are required for calculating the error in the volume conductivity measurements originating from surface leakage conductances [19]. A Hitachi scanning electron microscope of type S-4100 with field emission electron source was used for investigating the specimen surfaces.

The 4 cm diameter specimen holder was bolted tightly to a temperature-controlled nickel block. The thermocouple was positioned in the holder, about 1 mm below the specimen. The central part of the specimen (using a 3 mm and in one case an 8 mm beam aperture) was irradiated by 28 MeV alpha particles which have a range of about 210 μm in alumina and thus are basically all deposited beyond the specimen, into the brazing foil. During irradiation an electric field of about 350 V/mm was applied across the specimens, and the temperature at the specimen was kept at 450 or 500°C. Further details on the irradiation parameters are found in Ref. [19].

The resistance R between central and base electrode was measured, while the alpha particle beam was turned off, using a Keithley 6517 electrometer. In frequent intervals the resistances between central and guard electrode R_{PG} and guard and base electrode R_G were also measured, together with the resistance R_{cG} of contact plus lead to the guard electrode. The latter is about half the resistance measured between the two independent leads to the guard electrode. Independent of whether a guard ring is used or not, the measured volume conductance $1/R_P^{meas}$ consists of the true volume conductance $1/R_P$ and a contribution $\Delta(1/R)$ resulting from surface leakage currents [19],

$$\frac{1}{R_P^{meas}} = \frac{1}{R_P} + \Delta\left(\frac{1}{R}\right). \tag{1}$$

$\Delta(1/R)$, which in an unguarded experiment is simply the surface conductance, in an electrically guarded experiment can in most cases be approximated by [19]

$$\Delta\left(\frac{1}{R}\right) = \frac{R_{cG}}{R_{PG} R_G}. \tag{2}$$

3. Electrical surface conductance

From transmission (TEM) and scanning (SEM) electron microscopy the phenomenon of radiation-induced contamination of specimen surfaces is well known. The phenomenon can be best visualized when the situation for a finely focussed electron beam in a TEM is considered. Narrow, spire-like agglomeration of carbon contamination builds up within the specimen area which is hit by the electron beam as indicated in Fig. 1. On the back side of the thin TEM specimens a rounded and somewhat lower contamination spike occurs. The contamination originates from hydrocarbon molecules which have two possible sources. In an only moderately high vacuum (typically less than 10^{-5} Torr) it predominantly originates from the residual hydrocarbon partial pressure in the specimen envi-

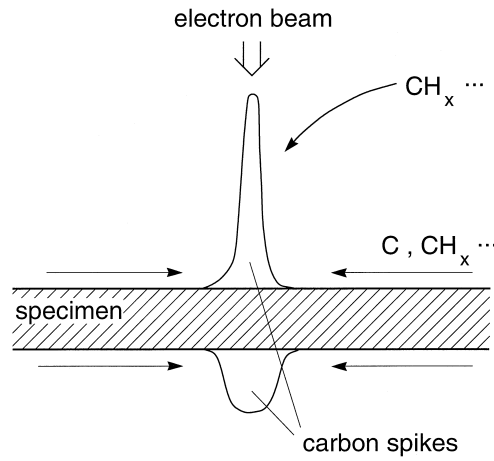

Fig. 1. Carbon contamination spikes as generally observed in focussed electron beam TEM. Arrows indicate the influx of hydrocarbon molecules from the specimen surface and from residual gas in the vacuum.

ronment. The hydrocarbon molecules are cracked by the fast particle beam and carbon-rich residues are deposited on the specimen surface. On the other hand, contamination spikes are observed also under high vacuum conditions owing to hydrocarbon impurities present on specimen surfaces. Under the influence of the electron beam (possibly due to the temperature gradient) the hydrocarbon molecules on the specimen surface migrate towards the irradiated specimen area where they are cracked and pinned by the electron beam. A side effect of this surface migration is that the surface areas in the vicinity of the irradiation spot are cleaned of contaminants.

Both effects, increase of contamination in the irradiated specimen area and decrease in the area surrounding the irradiated one, have been identified in the conductivity measurements of the present ion irradiation experiments in search for RIED as is revealed in Fig. 2. Both results shown in this figure have been obtained in the same type of alumina (Rubalit 710) during alpha particle irradiation at 500 to 550°C. Fig. 2(a) reveals an increase of the apparent electrical conductivity due to the ion irradiation-induced surface contamination when the insulating ring between central and guard electrode was included in the area which was irradiated by the ion beam. The sudden decrease of conductivity at the end of the irradiation included in Fig. 2(a) is due to post-irradiation treatment. After the irradiation the surface film was oxidized by heating the specimen to 500°C in air, and the bulk conductivity of Rubalit alumina of about $4 \times 10^{-11}\,(\Omega\ \mathrm{m})^{-1}$ was restored.

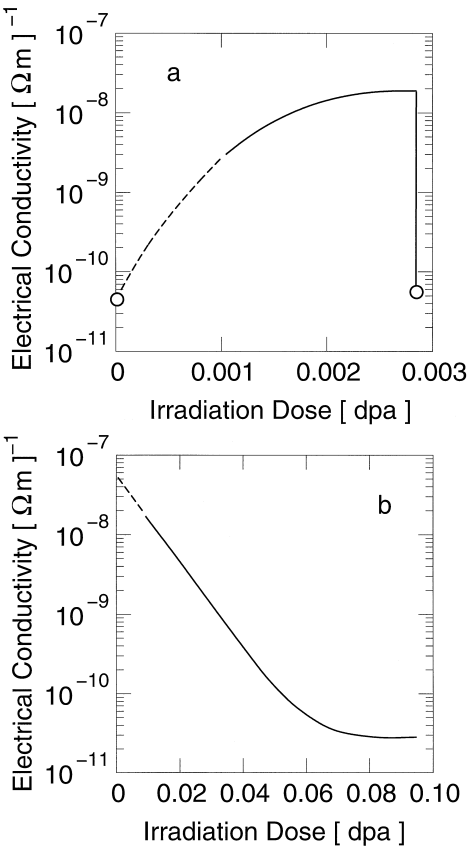

Fig. 2. Apparent electrical conductivity measured as a function of irradiation dose in Rubalit type Al_2O_3, irradiated at 500°C. (a) Increase and (b) decrease of apparent conductivity owing to radiation-induced increases and decreases, respectively, of surface conductance.

Fig. 2(b) shows a decrease of the apparent electrical conductivity when only part of the center electrode was irradiated. The high starting conductivity in this case results from pre-irradiation contamination of the sample. During irradiation original contamination from the insulating ring between central and guard electrode was dragged into the irradiated area on the central electrode. In both cases (shown in Fig. 2(a) and (b)) it was checked by measuring R_{PG}, R_G and R_{cG}, and inserting the values into Eqs. (1) and (2) that the conductivity changes were due to surface and not to bulk conductivity changes. It is concluded that the situation in fast particle irradiation experiments is analogous to the situation in transmission and scanning electron microscopes where the contamination layers have been directly observed in the microscope.

The existence of such radiation-dominated carbon contamination requires special precautions against surface leakage conductances when electrical conductivity measurements are performed on irradiated specimens. Application of the guard ring technique is mandatory (some previous RIED experiments have unfortunately been performed without a guard ring). Nevertheless, even when the guard ring is applied, high apparent conductivity increases resembling the RIED effect but originating from surface leakage currents have been observed [15].

On the other hand RIED may be of concern as a radiation-induced surface conductivity effect, and the impact of 'surface RIED' for the design of electrically insulating fusion reactor components needs to be studied in the future.

4. Electrical conductance through microcracks

Owing to the low ductility of electrical insulator oxide ceramics and to their decreasing strength with decreasing impurity content, the danger for crack formation is high in typical RIED experiments, where the ceramic specimens have to be solidly bonded to sufficiently good heat conducting (metallic) specimen holders. Microcracks can arise because of the temperature cycling during brazing or irradiation due to the differential thermal expansion of specimen and specimen holder. They may, however, also originate from grinding and polishing during specimen preparation. Both single and polycrystalline specimen materials

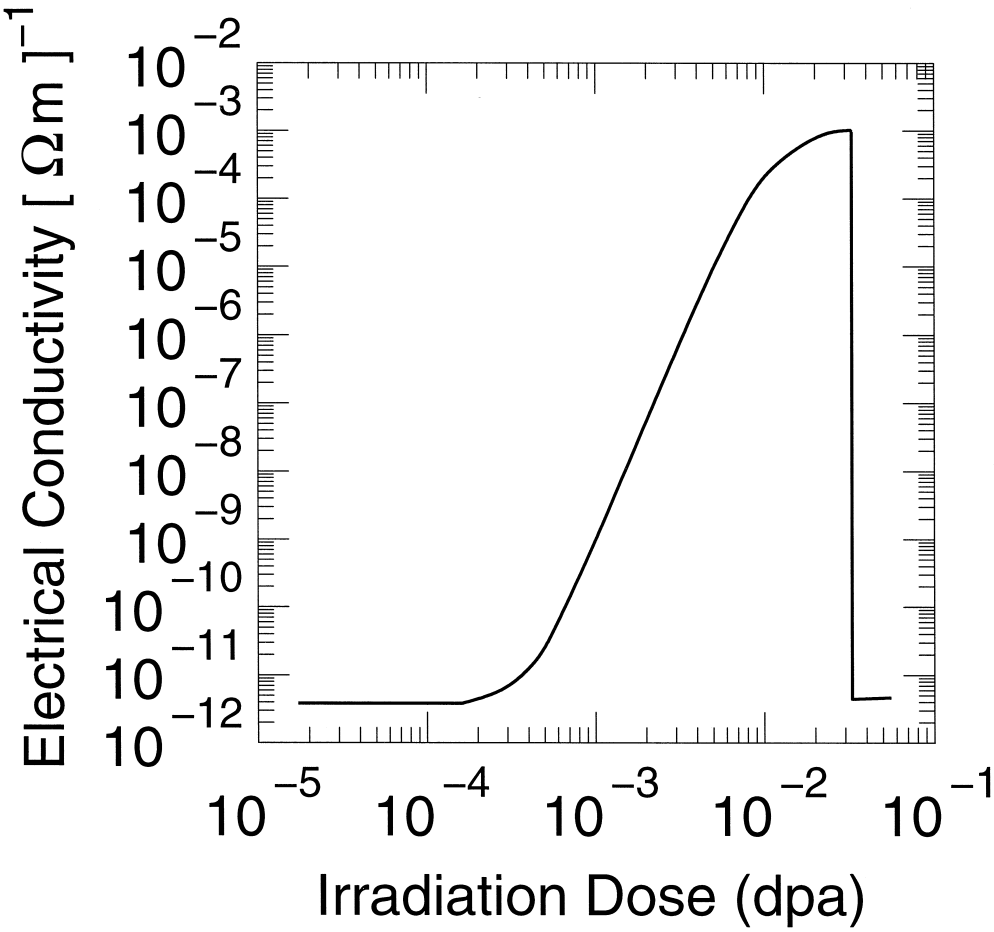

Fig. 3. Apparent electrical conductivity measured as a function of irradiation dose in single crystal Al_2O_3, irradiated at 450°C. The RIED-like increase of the electrical conductivity is caused by leakage currents along microcracks. Restoration of the pre-irradiation conductivity value was achieved by a short increase in temperature and dose rate.

used in the present study were of high purity and thus prone to such microcracking.

The single crystal, used for the measurements in Fig. 3, was brazed onto a nickel holder. Nickel has a relatively high heat conductivity but a thermal expansion coefficient which is 50% higher with respect to that of alumina. The specimen was alpha particle irradiated in vacuum of $\leq 1.5 \times 10^{-6}$ Torr at 450°C. (The thermocouple, positioned 1 mm below the specimen, was held at 430°C resulting in a specimen temperature of (450 ± 10)°C during irradiation.) The alpha particle current measured at the specimen was 1×10^{-6} A, i.e. the current density was 1.4×10^{-5} A/cm^2, corresponding to a displacement damage rate of 1×10^{-6} dpa/s and ionizing dose rate of 1.7×10^6 Gy/s. (The heat deposition into the specimen and brazing foil is 28 J/s.) The electrical conductivity, measured with alpha particle beam off, is shown in Fig. 3 as a function of displacement dose. After some incubation time a rapid increase of the electrical current by many orders of magnitude is observed. The behaviour is similar to previously reported RIED results, but is not attributed to volume conductivity increases.

After 0.8×10^{-3} dpa the surface conductance term (as determined from R_{PG}, R_G, and R_{cG} via Eq. (2)) had grown from 0.3×10^{-16} to 1×10^{-16} Ω^{-1} and then remained constant up to the final irradiation dose. Comparing this to the measured conductance values of between 10^{-4} and 10^{-12} Ω^{-1}, reveals that surface leakage conductance (external leakage) did not play a role throughout the whole experiment.

From our previous investigations on unirradiated specimens, the existence of microcracks (as was verified in subsequent post-irradiation investigations, see below) was expected, and leakage conductance along the surfaces of the microcracks (internal leakage) was anticipated to be responsible for the observed conductivity increase. Therefore, before terminating the irradiation experiment, an attempt was made to influence the electrical properties of

the surfaces inside the microcracks by changing the thermal and stress conditions in the specimen via altering the accessible irradiation parameters. At a dose of 3.6×10^{-2} dpa the temperature was first raised to 600°C for a few minutes and then the dose rate was doubled for a few minutes. The result was an almost abrupt decrease of the conductivity down to the pre-irradiation value (see Fig. 3). During further dose increase under the original irradiation conditions at 450°C to a final dose of 4.5×10^{-2} dpa the conductivity remained unaltered at its pre-irradiation value. Repetition of the experiment on a specimen, that revealed no microcracks, showed no conducitivity increase [20].

Occurrence and shape of microcracks were investigated by SEM. Fig. 4 shows a microcrack in a Vitox specimen after brazing it by Ag–Cu–In–Ti foil to a Vacon70 specimen holder. The thermal expansion coefficient of the Vacon70 alloy is close to that of alumina. The crack of about 1 μm width had been introduced by the cooling from 950°C (brazing temperature) to room temperature. Thus even when Vacon70 specimen holders are used microcracks may occasionally occur, and control for microcracks is always required. The crack in the polycrystalline specimen (Fig. 4) had grown along grain boundaries. Branching of the crack at a grain boundary junction has led to a side crack of less than 0.1 μm width which can be clearly recognized by the present method when imaged with only 1 kV accelerating voltage.

An image of a microcrack, which was taken after the Ti and Au contact layers had been attached, is shown in Fig. 5. The crack is clearly visible. The metal layer, however, covers fine details. Finally Fig. 6 shows a crack in an irradiated specimen. (It is the same specimen, the electrical conductivity evolution of which is shown in Fig. 3.) In this specimen a high resistance of $> 10^{15}$ Ω was maintained after irradiation also when the specimen had been cooled to room temperature. The micrograph shows that as an effect of irradiation some material has been heaped up to both sides of the crack, and at the same time the edges between crack surface and outer surface have been rounded off. This restructuring of material on the specimen surface is caused by the high-temperature irradiation. It could possibly be related to the observed restoration of the electrically insulating properties which had occurred in this specimen (Fig. 3). The electrical conductivity had been restored even though the cracks were still visible in SEM (Fig. 6).

Figs. 4–6 show that a sensitive method for microcrack identification, either pre- or post-irradiation, is achieved via secondary electron imaging using low accelerating voltages. In order to apply this method, the specimen surfaces need to be polished before attachment to the specimen holder. The method of SEM inspection is sensitive, but time consuming. Since an SEM frame, preferably chosen at a magnification of 5000 to 7000, covers only an area of about 10 μm by 10 μm, a raster including several thousand frames needs to be inspected even for covering only the central part of the specimen which has been irradiated or is intended for later irradiation.

The present results show that large conductivity increases can occur under irradiation as a result of micro-

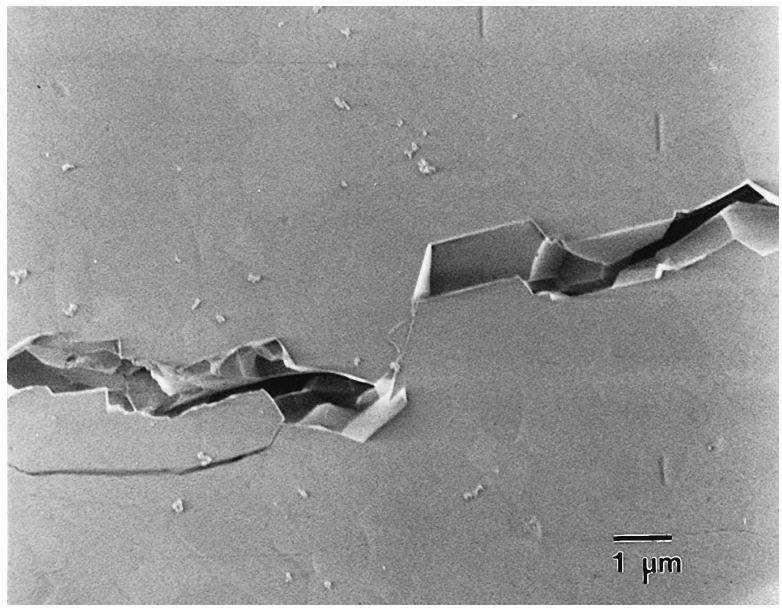

Fig. 4. SEM secondary electron image (acceleration voltage 1 kV) of a 1 μm wide microcrack in an unirradiated polycrystalline Al_2O_3 specimen. A branch of the crack, only about 0.05 μm wide, reveals the high sensitivity of the method.

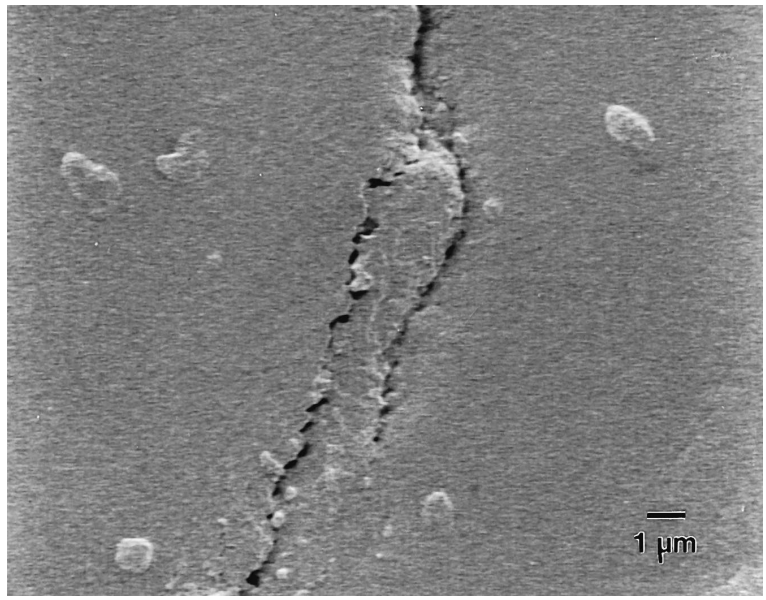

Fig. 5. SEM image (acceleration voltage 1 kV) of a microcrack in a single crystal specimen after sputter deposition of the metallic contact layer.

cracks. Since the conductivity increases are attributed to conducting paths along internal surfaces, no closed pores, but only interconnected cavities, microcracks or fissures, traversing through the specimen, are effective. On the other hand the results also show that microcracks, even when extending through the specimen, do not necessarily increase the conductivity under irradiation. Depending on the irradiation conditions microcracks may be healed or

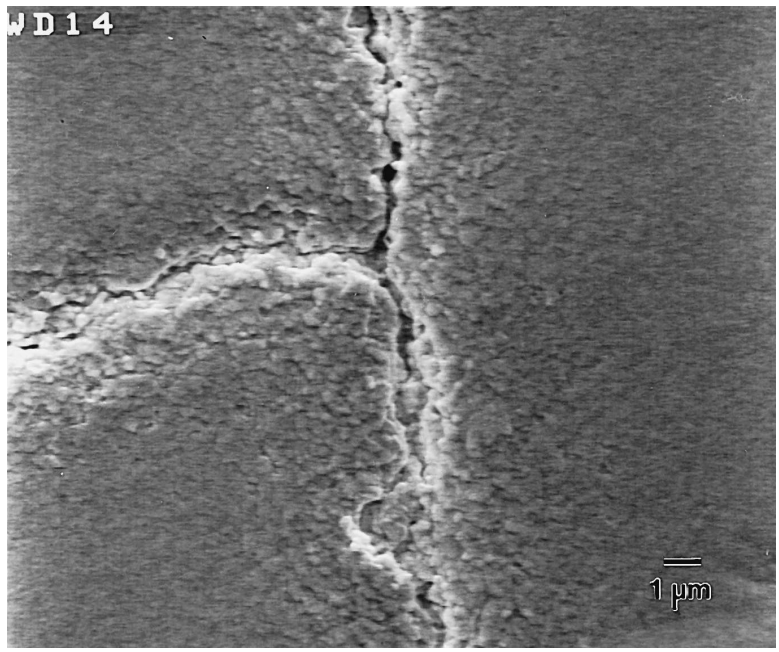

Fig. 6. The same specimen as in Fig. 3, post-irradiation SEM image of a microcrack. The irradiation has led to a visible amount of material restructuring at and near the microcracks.

sealed against the effect of radiation-enhanced surface conduction. In the present experiment the effective sealing of the existent cracks was reached by a thermal and dose rate excursion. The reason may have been solid rejoining of the crack surfaces due to the compressive stresses imposed on the specimen while cooling back to 450°C. Pressed at elevated temperature between oxide crystals, the conductive film on the crack surface may have lost conductivity (e.g. by oxidation) or its atoms may have dissolved into the Al_2O_3 matrix. Another explanation might have been volatization of the conductive films from the crack surfaces at 600°C. This is unlikely however, since it would not have created a healing effect but should have led to a reproducible condition, i.e. the irradiation, which was continued by a further dose increment of 0.9×10^{-2} dpa after restoration of the pre-irradiation conductivity (see Fig. 3), should have led again to a conductance increase. (More than seven orders of magnitude conductance increase were originally observed at 0.9 dpa.)

Adverse effects of cracks and grain boundary conduction on RIED measurements had already been discussed in three previous publications. Zinkle et al. found apparent conductivity increases in amorphous alumina films, which were sputtered onto tantalum substrates, due to radiation-induced microcracks [21]. Patuwathavithane et al. observed apparent conductivity increases due to radiation-enhanced diffusion of gold electrode material along grain boundaries [25]. Finally Wedig observed significant conductance increases (up to seven orders of magnitude, in vacuum and in air) even without irradiation in specimens containing microcracks, while no conductance increases were observed in control measurements on specimens without cracks [22]. Also the large apparent RIED effect originally reported by Möslang et al. [23] could later be attributed to fractures through the specimen, and a repetition of the latter experiment showed no conductivity increase [25]. It is suggested that also other experiments, from which the occurrence of bulk RIED was inferred, should be repeated with attention paid to the presence of fractures or microcracks.

The reason for the high radiation-driven increase of 'internal' surface conductance as observed by Möslang et al. and in the present work needs to be studied, and it is further necessary to investigate whether the effect of radiation-enhanced internal leakage conductance plays a role in macroscopic components for fusion reactor design.

5. Conclusion

The validity of the electrical guard technique in measurements of the electrical conductivity in Al_2O_3 has been tested under alpha particle irradiation. Depending on the particle beam diameter, increases as well as decreases of the apparent bulk conductivity have been observed as a result of 'external' surface leakage currents. They are explained by radiation-modified surface contamination. It is concluded that in measurements of the electrical bulk conductivity of highly insulating materials the contribution from surface leakage conductance has to be determined, and may be calculated from the measured values of two surface resistances (R_{PG}, R_G) and one of the contact resistances (R_{cG}).

Large increases of the apparent bulk conductivity were observed also as an effect of radiation-enhanced 'internal' surface conductance through microcracks. Sealing of the cracks resulting in a reversal of this conductivity increase was obtainable by changing the irradiation conditions. Hence the occurrence of microcracks can be the second reason of a systematic error in bulk conductivity measurements. Inspection for microcracks by SEM on pre-polished specimens is recommended. It is shown that surface cracks of less than 0.1 μm width can be identified by this method.

In search for RIED, experiments by several research groups have recently been performed with standardized experimental conditions (control of R_{PG}, R_G, and R_{cG}, as defined at the IEA workshop in Stresa, 1993) [19,22,24–29]. None of these experiments did confirm the existence of permanent bulk conductivity increases. It needs to be verified that previous RIED-like effects in electron, proton, and neutron irradiation have not been caused by either surface or microcrack leakage conductances. Unless the earlier RIED results can be reconfirmed in repeating those experiments under the now standardized conditions including measurement of contact and surface resistances and (where applicable) post-irradiation tests for microcracking, it has to be assumed that RIED as a bulk effect does not exist or else exists only under very special conditions.

Electrical leakage conductances, both along the outer specimen surface as well as through microcracks in the specimen interior, can be radiation-enhanced by many orders of magnitude. Thus RIED as an effect of radiation-enhanced surface conductivity needs to be further investigated, and the impact of 'surface RIED' on electrically insulating fusion reactor components needs to be studied. In these studies outer surfaces as well as cracks within the components need to be taken into consideration.

Acknowledgements

The author would like to thank W. Schmitz for his assistance with the irradiation and SEM and J. Deutz for the specimen preparation.

References

[1] R.W. Klaffky, B.H. Rose, A.N. Goland, G.J. Dienes, Phys. Rev. B 21 (1980) 3610.
[2] E.R. Hodgson, Cryst. Latt. Def. Amorph. Mater. 18 (1989) 169.

[3] E.R. Hodgson, J. Nucl. Mater. 179–181 (1991) 383.
[4] E.R. Hodgson, Proc. 12th Int. Conf. Defects in Insulator Materials, Nordkirchen, 1993, p. 332.
[5] E.R. Hodgson, J. Nucl. Mater. 212–215 (1994) 1123.
[6] A. Morono, E.R. Hodgson, J. Nucl. Mater. 212–215 (1994) 1119.
[7] G.P. Pells, E.R. Hodgson, J. Nucl. Mater. 226 (1995) 286.
[8] X.-F. Zong, C.-F. Shen, S. Liu, Z.-C. Wu, Y. Chen, Y. Chen, B.D. Evans, R. Gonzalez, C.H. Sellers, Phys. Rev. B 49 (1994) 15514.
[9] X.-F. Zong, C.-F. Shen, S. Liu, Z.-C. Wu, Y. Chen, R. Zhang, J.G. Zhu, Y. Chen, B.D. Evans, R. Gonzalez, C.H. Sellers, J. Nucl. Mater. 219 (1995) 176.
[10] X.-F. Zong, C.-F. Shen, S. Liu, Y. Chen, R. Zhang, Y. Chen, J.G. Zhu, B.D. Evans, R. Gonzalez, Phys. Rev. B 54 (1996) 139.
[11] G.P. Pells, J. Nucl. Mater. 184 (1991) 177.
[12] G.P. Pells, B.C. Sowden, J. Nucl. Mater. 184 (1991) 177.
[13] T. Shikama, M. Narui, Y. Endo, T. Sagawa, H. Kayano, J. Nucl. Mater. 191–194 (1992) 575.
[14] T. Shikama, M. Narui, H. Kayano, T. Sagawa, J. Nucl. Mater. 212–215 (1994) 1133.
[15] W. Kesternich, F. Scheuermann, S.J. Zinkle, J. Nucl. Mater. 206 (1993) 68.
[16] A. Möslang, private communication.
[17] P. Jung, Z. Zhu, H. Klein, J. Nucl. Mater. 206 (1993) 72.
[18] E.H. Farnum, F.W. Clinard, J. Nucl. Mater. 219 (1995) 161.
[19] W. Kesternich, F. Scheuermann, S.J. Zinkle, J. Nucl. Mater. 219 (1995) 190.
[20] W. Kesternich, to be published.
[21] S.J. Zinkle, J.H. Hunn, R.E. Stoller, Mater. Res. Soc. Symp. Proc. 373 (1995) 299.
[22] F. Wedig, PhD thesis, Forschungszentrum Jülich, Report 3334, 1996.
[23] A. Möslang, E. Daum, R. Lindau, Proc. 18th Symp. Fusion Technology, Karlsruhe, 1994.
[24] A. Möslang, IEA Workshop on Radiation Effects in Ceramic Insulators, ORNL/M-6068, Cincinnati, OH, May 8–9, 1997.
[25] C. Patuwathavithane, W.Y. Wu, R.H. Zee, J. Nucl. Mater. 225 (1995) 328.
[26] L.L. Snead, D.P. White, S.J. Zinkle, J. Nucl. Mater. 226 (1995) 58.
[27] E.H. Farnum, T. Shikama, M. Narui, T. Sagawa, K. Scarborough, J. Nucl. Mater. 228 (1996) 117.
[28] L.L. Snead, D.P. White, W.S. Eatherly, S.J. Zinkle, Fusion Reactor Semianual Prog. Rep., DOE/ER-0313/19, 1996.
[29] S.J. Zinkle, W.S. Eatherly, L.L. Snead, T. Shikama, K. Shiiyama, Fusion Reactor Semianual Prog. Rep., DOE/ER-0313/22, 1997, p. 188.